

Momentum-transfer dependence of Fano parameters for the $(1s^2)^1S \rightarrow (2s2p)^1P$ doubly excited transition in helium

X W Fan and K T Leung

Department of Chemistry, University of Waterloo, Waterloo, Ontario N2L 3G1, Canada

E-mail: tong@uwaterloo.ca

Received 23 October 2000

Abstract

We report the first detailed characterization of absolute generalized oscillator strength (GOS) of the $(1s^2)^1S \rightarrow (2s2p)^1P$ doubly excited transition in helium as a function of momentum transfer (K) by angle-resolved electron energy loss spectroscopy at 2.5 keV impact energy. The GOS profile is found to be dominated by a strong maximum at $K = 0$, characteristic of dipole-dominated interactions. Extrapolating our GOS profile to $K = 0$ using a semi-empirical power series (Lassette series) gives an absolute OS of 0.0052, in good accord with theoretical and experimental optical values reported in the literature. Changes in the Fano parameters for the doubly excited transition are determined for the first time as a function of momentum transfer. The Fano profile index (q) increases rapidly from -2.75 in the $K = 0$ limit (observed earlier optically) to -1.5 at $K^2 \sim 1.5$ au and levels off to -1.0 at $K^2 \sim 4$ au, while the Fano correlation coefficient (ρ^2) decreases slowly from 0.04 at $K \sim 0$ to 0.03 at $K^2 \sim 4$ au. These variations reflect the intricate nature of the transition matrix elements involved in the interference between direct ionization and autoionization. Finally, we also obtain clear evidence for the presence of a non-dipole autoionizing resonance near 58.1 eV in He in the higher- K region, confirming an earlier theoretical prediction.

Autoionization may occur when neutral atoms are excited to energy levels above their first ionization limits [1–3]. The autoionization states have continued to attract considerable interest because such high-lying states require the simultaneous excitation of two electrons, providing a unique opportunity to study electron correlation and interference effects arising from competition with the direct ionization channel in these doubly excited electronic states. The simplest system that exhibits autoionizing states is helium, which therefore provides an important benchmark system for both theoretical and experimental investigations into these intricate phenomena. The existence of doubly excited autoionizing resonances in helium was first discovered by Whiddington and Priestley using electron impact at 100–600 eV in 1934

[4], and later characterized by photoabsorption [5–7] and other electron scattering techniques [8–10]. In spite of the wealth of information on this system, most of the spectroscopic studies to date have focused on the determination of resonance energies and other autoionizing resonance parameters at the optical or zero-momentum transfer limit. Unlike optical studies where the resonances are governed by the dipole selection rules, electron impact work offers the prospect of accessing non-dipole excitation processes involving optically forbidden autoionization transitions. Furthermore, the Fano parameters can be determined as a function of momentum transfer to provide new insights into these important fundamental processes.

Lassetre and co-workers have pioneered the use of angle-resolved electron energy loss spectroscopy (EELS) for precise absolute measurements of the generalized oscillator strength (GOS), thus providing quantitative information on both dipole-allowed and non-dipole transitions [11]. The GOS is defined as [12]

$$f(K, E) = \frac{E}{K^2} \left| \left\langle \Psi_n \left| \sum_{j=1}^N \exp(i\mathbf{K} \cdot \mathbf{r}_j) \right| \Psi_0 \right\rangle \right|^2 \quad (1)$$

where Ψ_0 and Ψ_n are the (N -electron) electronic wavefunctions of the initial (ground) and final states, respectively; and \mathbf{r}_j is the position of the j th electron with respect to the centre of mass of the target. The GOS profile (over an extended range of momentum transfer \mathbf{K}) of an individual transition at an energy loss E therefore provides a detailed ‘mapping’ of the overlap function between the initial-state and final-state wavefunctions in momentum space, which can be used for spectral assignments, theoretical modelling of the excited-state wavefunctions, and better understanding of the nature of underlying interactions [13]. Despite the inferior energy resolution in high-energy electron scattering work relative to photon impact techniques, the development of angular sampling (i.e. as a function of the scattering angle or momentum transfer) has opened up a new window into dipole-forbidden phenomena that are not easily accessible by optical techniques.

Only two of the early studies of doubly excited autoionizing resonances in helium attempted to examine angular or momentum-transfer dependent effects. In particular, Silverman and Lassetre determined differential GOS at three selected energy losses (58.9, 60.0 and 61.3 eV), over a limited momentum transfer range of 0.3–1.0 au at an impact energy of 500 eV [8]. Indeed, this work provided the first detailed lineshape measurement that stimulated much of the theoretical work on the dynamics of multiply electron excitations in atoms by Fano and co-workers [1–3]. Using a 25 keV impact energy, Wellenstein *et al* reported EELS observation of resonance-like structure at an energy loss of 60 eV out to a momentum transfer of 4 au [9]. Although the low energy resolution (2 eV FWHM) precluded the authors from ruling out contributions from some of the optically forbidden transitions, Wellenstein *et al* alluded to the possible interest and significance in the momentum-transfer dependence of the Fano parameters in these doubly excited transitions [9]. In this paper, we present a detailed characterization of the absolute GOS profile of the He $1s^2 \rightarrow 2s2p$ transition by using EELS at 2.5 keV impact energy, and illustrate the intricate changes in the Fano parameters as functions of the momentum transfer for the first time. Our measurement also provides clear evidence for the presence of a non-dipole doubly excited autoionization resonance at 58.1 eV.

Details of the theoretical background and the instrumentation technique used in our laboratory for angle-resolved EELS have been given elsewhere [14]. Briefly, a collimated electron beam was accelerated to an impact energy of 2.5 keV and crossed with a gas jet expanded from a nozzle (0.5 mm diameter) positioned 1 cm above the collision centre. Electrons scattered with an energy loss E at a scattering angle θ (from the forward direction)

were energy-analysed using a hemispherical energy analyser equipped with a seven-element input lens. Our spectrometer was capable of an optimal energy resolution of 0.7 eV FWHM and an angular resolution of 0.2° half-angle. The angular divergence of the beam in our spectrometer has been improved with smaller defining apertures. The gas cell has also been upgraded with a cylindrical cage to provide a more uniform, higher gas density at the collision centre and to further minimize stray field. These minor modifications, along with the use of a higher gain electron multiplier, provide marked improvements to the signal-to-background performance and overall collection efficiency of our spectrometer.

EELS spectra were collected over an energy loss range of 4–160 eV at a series of θ angles from 1.5° to 8.5° in steps of 0.5° (corresponding to different momentum transfers) sequentially in repetitive scans. After each measurement of the sample gas introduced to the centre of the collision chamber (sample spectra), EELS spectra of the sample gas introduced outside the collision cell at the same pressure ($1\text{--}2 \times 10^{-5}$ Torr) were recorded in the same energy loss and angular ranges (ambience spectra). Contributions from the ambient gas were removed by subtracting the corresponding ambience spectra from the sample spectra after appropriate normalization. The experimental relative cross section in the resulting EELS spectra was converted to relative GOS using the Bethe–Born formula, which in Rydberg atomic units can be written as [12]

$$\frac{df(K, E)}{dE} = \frac{k_0 K^2 E}{k} \frac{d^2\sigma}{4 d\Omega dE} \quad (2)$$

where $d\Omega$ is the detection solid angle, E is the energy loss, k_0 and k are the momenta of the incident and scattered electrons, respectively, and $K (= k_0 - k)$ is the momentum transfer. Because the EELS spectra were collected in a relatively normalized fashion, the entire relative GOS data could be put on an absolute scale by applying the Bethe-sum-rule normalization to a Bethe–Born-corrected EELS spectrum collected at a single momentum transfer [12]:

$$\int \frac{df(K, E)}{dE} dE = N \quad (3)$$

where N is the total number of electrons in the target. In the Bethe-sum-rule normalization procedure, the intensity of the relative GOS obtained at a particular momentum transfer was numerically integrated over the sampling energy loss range (160 eV in the present case), while the remaining intensity from 160 eV to infinity was estimated by integration of a fitted function $B(E) = A/E^\nu$, where the empirical constants A and ν were obtained by curve fitting $B(E)$ to the experimental data between 70 and 160 eV. The sum of these two integrated intensities was then normalized to the total number of electrons (2) in He.

The angular scale was calibrated by comparing the GOS profiles of the $1s^2 \rightarrow 1s2s$ and $1s^2 \rightarrow 1s2p$ transitions in He with the corresponding theoretical calculations [15], and independently verified by applying the Bethe-sum-rule normalization procedure at several selected scattering angles near the forward scattering direction. No geometrical correction was found to be necessary for the ‘short’ experimental angular range and the high impact energy employed in this paper.

Figure 1 summarizes the measured EELS spectra as a function of energy loss and momentum transfer in the form of a Bethe surface [12]. The increasing dependence of the energy loss on K for a constant scattering angle is quite apparent for EELS spectra obtained at the larger angles, which increasingly skew towards the higher K direction. In addition to generally confirming the differential cross section measurements made at two angles by Wellenstein *et al* [9], the Bethe surface shown in figure 1 reveals the K dependence of the overall structure in the 50–70 eV region, which has already been found to be richly populated by

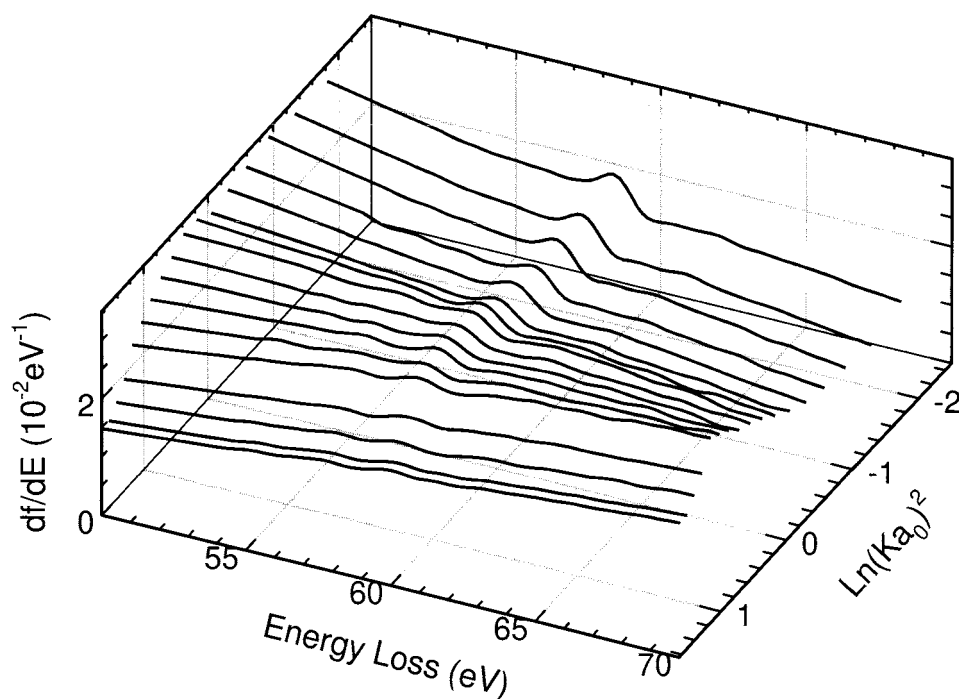


Figure 1. Bethe surface of the double excitation region of helium measured at 2.5 keV impact energy.

series of Fano resonances by high-resolution photoabsorption spectroscopy [7]. The changes in the shapes of the Fano profiles in this energy region are particularly interesting and point to the existence of slowly varying transitions characteristic of non-dipole excitation.

Figure 2 depicts selected EELS spectra measured at θ angles of 1.5° , 3° , 5° and 8° . These spectra have been appropriately normalized with respect to one another and made absolute individually using the Bethe-sum-rule normalization procedure. Three discernible spectral features have been identified at 58.1 eV (feature 1), 60.2 eV (feature 2), and 63.7 eV (feature 3). Following the high-resolution ejected electron energy spectroscopic studies of Oda *et al* [16] and Hicks and Comer [17] at low impact energies, the weak feature 1 can be attributed to a mixture of two close-lying resonances ($2s^2$) 1S at 57.9 eV and ($2s2p$) 3P at 58.3 eV, which cannot be resolved with our limited energy resolution. Of particular interest is that feature 1 is clearly more intense at higher momentum transfers (e.g. $\theta = 5^\circ$ spectrum in figure 2(c)) than $K = 0$ (cf $\theta = 1.5^\circ$ spectrum in figure 2(a)). This intensity variation provides the strongest evidence to date for the presence of a non-dipole Fano-type transition, which is consistent with the early assignment of the ($2s^2$) 1S resonance at 57.9 eV [16, 17]. This work therefore provides the first observation of a non-dipole doubly excited transition by means of the momentum-transfer dependence of the GOS of the transition. Unlike feature 1, both features 2 and 3 appear to have stronger intensity near $K = 0$, indicative of the underlying dipole-dominated transitions. The most prominent feature (feature 2) at 60.2 eV displays the ‘classic’ Fano lineshape as described by the Fano formula (equation (4) below) and is assigned predominantly as the ($2s2p$) 1P doubly excited autoionizing resonance. The contribution from the non-dipole ($2p^2$) 1D resonance at 59.9 eV [16, 17] to the strong ($2s2p$) 1P resonance at 60.2 eV is expected to be negligible near $K = 0$. Like feature 2, the weak autoionizing ($2s3p$) 1P resonance at 63.7 eV (feature 3) is

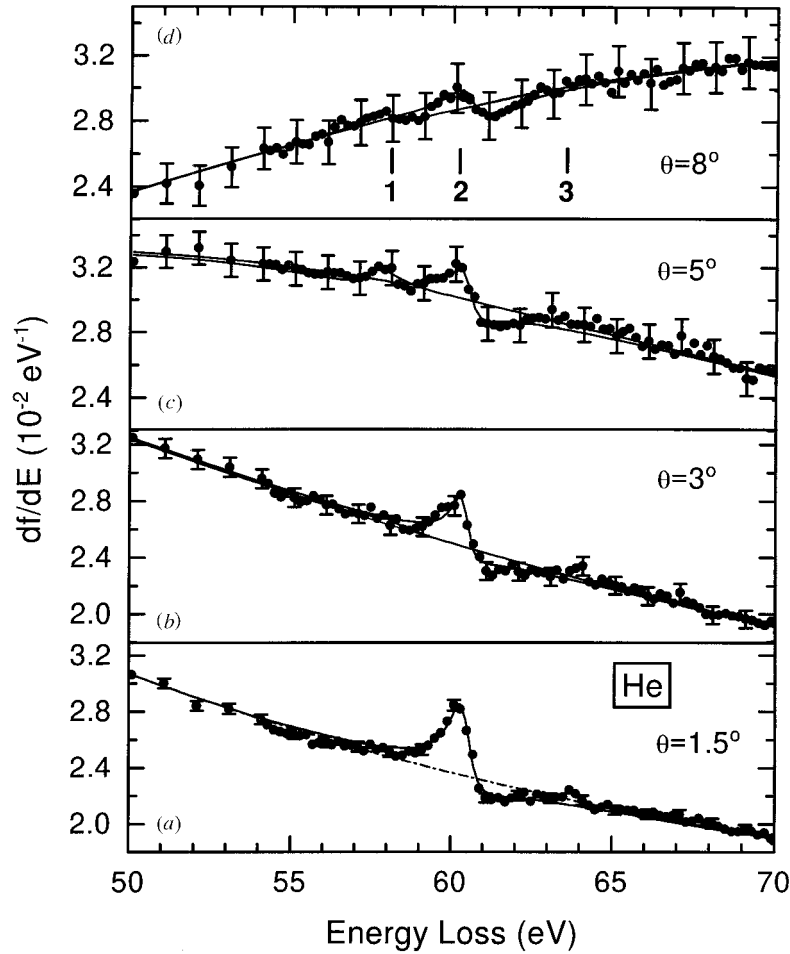


Figure 2. Angle-resolved electron energy loss spectra of helium measured at the scattering angles of (a) 1.5°, (b) 3.0°, (c) 5.0° and (d) 8.0°. The GOS in each spectrum has been made absolute using the Bethe-sum-rule normalization procedure. Two Fano profiles (full curves) have been used to estimate the intensities of feature 1 (58.1 eV) and feature 2 (60.2 eV). The non-resonant cross section is represented by a chain curve in (a).

found to be most intense at zero scattering angle, suggesting a similar predominantly dipole behaviour.

Fano provided the first quantitative interpretation of autoionization resonances in helium for the case of an isolated resonance interacting with one or more continuum states [1, 2], by parametrizing the total cross section σ_T in terms of the non-resonant cross section σ_0 and the so-called profile index q and correlation coefficient ρ^2 , as follows:

$$\sigma_T = \sigma_0 \left[\rho^2 \frac{(q + \varepsilon)^2}{1 + \varepsilon^2} + 1 - \rho^2 \right] \quad \varepsilon = \frac{E - E_0}{\Gamma/2} \quad (4)$$

where the reduced energy ε is defined in terms of the energy loss separation from the resonance energy E_0 and the linewidth Γ . Qualitatively, q governs the shape of the total cross section, and ρ^2 is a measure of the strength of the resonance. These parameters along with the linewidth are related to various matrix elements involving the initial state ψ_0 , a discrete state φ , and a set

of continuum states $\psi_{\alpha E}$ which interact with the discrete state in the double-electron excitation process. Fano and Cooper gave [2]

$$q = \frac{\langle \Phi | \mathbf{r} | \psi_0 \rangle}{\pi \langle \varphi | \mathbf{H} | \psi_{\alpha E} \rangle \langle \psi_{\alpha E} | \mathbf{r} | \psi_0 \rangle} \quad (5)$$

where \mathbf{H} is the appropriate Hamiltonian and \mathbf{r} is the dipole operator. The wavefunction Φ represents the discrete state modified by an admixture of states in the continuum. The parameter ρ can be thought of as the overlap integral between the continuum wavefunctions arising by autoionization and by direct ionization. These Fano parameters can be used to estimate the oscillator strength f for the $(2s2p)^1P$ resonance in He as follows [3]:

$$f = \frac{0.195}{\text{Ryd Mb}} q^2 \rho^2 \sigma_0 (\text{Mb}) \Gamma (\text{Ryd}). \quad (6)$$

To investigate the K dependence of the observed $(2s2p)^1P$ resonance at 60.2 eV, we have fitted the EELS spectra (in the form of an absolute differential cross section versus the energy loss) near the relevant energy loss region with two Fano lineshapes positioned at 58.1 and 60.2 eV to represent features 1 and 2, respectively. The experimental linewidth for feature 2 ($\Gamma = 0.73$ eV) was estimated from the EELS spectrum at 1.5° and is used as a fixed parameter for curve-fitting all the subsequent EELS spectra, while the Fano parameters (q and ρ^2) were treated as free parameters. The non-resonant cross section σ_0 was represented by a polynomial function fitted to the experimental cross section in the 45–55 eV and 65–80 eV regions (i.e. outside the immediate resonance region of interest). Figure 3(a) shows the resulting GOS profile for feature 2. Evidently, the GOS profile for the $(2s2p)^1P$ resonance is dominated by a strong maximum at $K = 0$, indicative of a dipole-dominated transition. The experimental GOS data are compared with the only K -dependent calculation available in the literature [18]. In particular, Froelich and Flores-Riveros reported a series of theoretical energy loss spectra at several momentum transfers [18], the GOS of which we estimated by using the fitting procedure discussed above. Although there is reasonable agreement between the experiment and the calculated GOSs for $K^2 < 0.5$ au, the calculated result appears to deviate substantially from our data at higher momentum transfer. The experimental GOS profile has also been fitted semi-empirically using the so-called Lassetre series [19]. The dipole oscillator strength estimated from extrapolation of the GOS data to zero momentum transfer using the Lassetre fit is found to be 0.0052, which is in good accord with the optical value inferred from the data of Madden and Codling (0.0057) [5] and from the calculations of Froelich and Flores-Riveros (0.0045) [18] and Salpeter and Zaidi (0.0050) [20].

Figures 3(b) and (c) show the fitted parameters defined in equation (4) used to obtain the GOS shown in figure 3(a). In keeping with the notion that the resonant contribution to the total cross section is very small for a doubly excited transition, figure 3(b) illustrates that the ratio of the non-resonant cross section to the total cross section converges to unity with increasing momentum transfer. Figure 3(c) shows that the profile index q increases rapidly from -2.75 in the $K = 0$ limit to -1.5 at $K^2 \sim 1.5$ au and levels off to -1.0 at $K^2 \sim 4$ au. In the $K = 0$ limit, our data clearly converge to the values estimated from optical data reported by Madden and Codling (-2.80) [5], Kossmann *et al* (-2.75) [6] and Schulz *et al* (-2.73) [7]. On the other hand, the correlation coefficient ρ^2 decreases slowly from 0.04 at $K \sim 0$ to 0.03 at $K^2 \sim 4$ au, suggesting that the overlap between the continuum wavefunctions from autoionization and direct ionization weakly depends on the momentum transfer. In deducing the Fano parameters, we have implicitly assumed the formalism developed by Fano and co-workers (equations (4)–(6)) [1–3], which is based on photon (dipole) excitation. While the present doubly excited transition is clearly predominantly dipole-allowed (as demonstrated

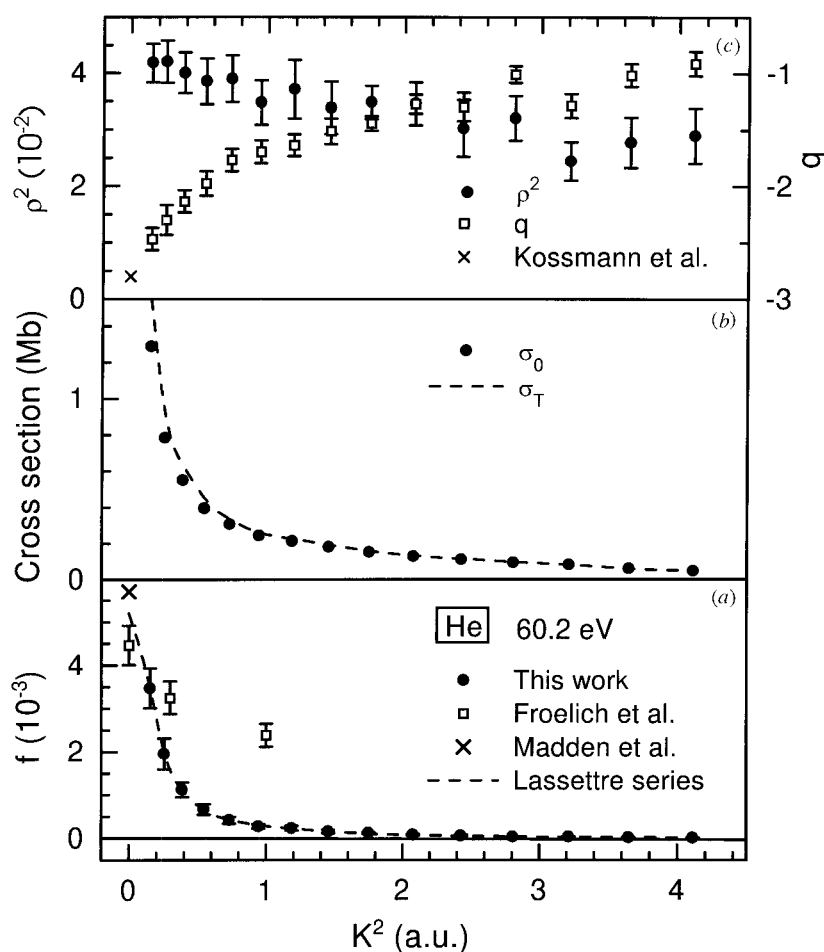


Figure 3. (a) Absolute generalized oscillator strength f , (b) total cross section σ_T and non-resonant cross section σ_0 , and (c) Fano profile index q and correlation coefficient ρ^2 are shown as functions of momentum transfer (K) squared for the He ($1s^2$) $^1S \rightarrow (2s2p)^1P$ doubly excited transition. Theoretical GOS data in (a) are obtained by applying the same curve-fitting procedure to the calculated spectra reported by Froelich and Flores-Riveros [18]. Only selected spectra that could be digitized reliably are used to estimate the corresponding GOS. The broken curve in (a) corresponds to a semi-empirical polynomial fit based upon the Lassetre series. The optical values for the oscillator strength in (a) and for the q parameter in (c) are obtained from Madden and Codling [5] and Kossmann *et al* [6], respectively.

by the GOS profile in figure 3(a)) and therefore the use of the dipole excitation formalism seems reasonable, further development of Fano's theory to include multipole excitation (as is possible with electron impact) is needed to put our approach on more comprehensive grounds. Such a theoretical development will address the important question of whether the momentum-transfer dependence in q and ρ^2 observed in this paper is due to kinematics effects (driven by the details of the electron collision process) or structural factors (that come from the transition matrix elements) or both.

In summary, we have determined absolute GOS of the two-electron ($1s^2$) $^1S \rightarrow (2s2p)^1P$ transition in He as a function of momentum transfer using angle-resolved EELS. The

experimental GOS profile converges to the dipole oscillator strength at the optical limit, while its momentum-transfer dependence clearly shows the underlying predominantly dipole interaction in this double electronic excitation. This paper also reveals possible inadequacies in an earlier calculation [18], particularly for modelling the higher momentum transfer region of the GOS, which underlines the theoretical challenges in modelling doubly excited states. That good agreement in resonance energies does not guarantee similar agreement in the GOS suggests that the GOS may provide a more sensitive probe for the wavefunctions involved. Furthermore, the present result demonstrates for the first time the intricate dependence of the Fano parameters on the momentum transfer and the potential of applying such a technique for probing the relevant transition matrix elements involved in the double and other multiple electronic excitation processes. Finally, this paper gives clear evidence for the presence of a non-dipole doubly excited transition at 58.1 eV at larger momentum transfer. We have very recently extended this paper on Fano parameters to the so-called window resonances in the 25–30 eV region of argon, which are found to exhibit similar momentum-transfer characteristics. Collectively, these data may provide new insights to the dynamics of multi-electron excitation processes and electron correlation effects.

Acknowledgment

This work was supported by the Natural Sciences and Engineering Research Council of Canada.

References

- [1] Fano U 1961 *Phys. Rev.* **124** 1866
- [2] Fano U and Cooper J W 1965 *Phys. Rev. A* **137** 1364
- [3] Fano U and Cooper J W 1968 *Rev. Mod. Phys.* **40** 441
- [4] Whiddington R and Priestley M 1934 *Proc. R. Soc. A* **145** 462
- [5] Madden R P and Codling K 1963 *Phys. Rev. Lett.* **10** 516
Madden R P and Codling K 1965 *Astrophys. J.* **141** 364
- [6] Kossmann H, Krassig B and Schmidt V 1988 *J. Phys. B: At. Mol. Opt. Phys.* **21** 1489
- [7] Schulz K, Kaindl G, Domke M, Bozek J D, Heimann P A, Schlachter A S and Rost J M 1996 *Phys. Rev. Lett.* **77** 3086 and references therein
- [8] Silverman S M and Lassetre E N 1963 *J. Chem. Phys.* **40** 1265
- [9] Wellenstein H F, Bonham R A and Ulsh R C 1972 *Phys. Rev. A* **8** 304
- [10] Chan W F, Cooper G and Brion C E 1990 *Phys. Rev. A* **44** 186
- [11] Lassetre E N and Skerbele A 1974 *Methods of Experimental Physics* vol 3, part B, ed D Williams (New York: Academic) p 868
- [12] Inokuti M 1971 *Rev. Mod. Phys.* **43** 297
- [13] Bonham R A 1979 *Electron Spectroscopy: Theory, Techniques and Applications* vol 3, ed C R Brundle and A D Baker (New York: Academic) p 127
- [14] Ying J F, Daniels T A, Mathers C P, Zhu H and Leung K T 1993 *J. Chem. Phys.* **99** 3390
- [15] Kim Y K and Inokuti M 1968 *Phys. Rev.* **175** 176
- [16] Oda N, Nishimura F and Tahira S 1969 *Phys. Rev. Lett.* **24** 42
- [17] Hicks P J and Comer J 1975 *J. Phys. B: At. Mol. Phys.* **8** 1866
- [18] Froelich P and Flores-Riveros A 1986 *J. Chem. Phys.* **86** 2674
- [19] Lassetre E N 1965 *J. Chem. Phys.* **43** 4479
Dillon M A and Lassetre E N 1975 *J. Chem. Phys.* **62** 2373
- [20] Salpeter E E and Zaidi M H 1962 *Phys. Rev.* **125** 248